A Novel Reverberation Chamber for In Vitro Bioelectromagnetic Experiments at 3.5 GHz

Rosa Orlacchio, Guillaume Andrieu, Alexandre Joushomme, Lorenza Patrignoni, Annabelle Hurtier, Florence Poulletier de Gannes, Isabelle Lagroye, Yann Percherancier, Delia Arnaud-Cormos, Philippe Lévêque

HAL Id: hal-04284652
https://cnrs.hal.science/hal-04284652

Submitted on 14 Nov 2023

A Novel Reverberation Chamber for *in Vitro* Bioelectromagnetic Experiments at 3.5 GHz

Rosa Orlacchio, Guillaume Andrieu, *Senior Member, IEEE*, Alexandre Joushomme, Lorenza Patrignoni, Annabelle Hurtier, Florence Poulletier De Gannes, Isabelle Lagroye, Yann Percherancier, Delia Arnaud-Cormos, *Member, IEEE*, Philippe Leveque, *Member, IEEE*

Abstract—In this study, a mode- stirred reverberation chamber (RC) was designed and proposed for the first time as a cell culture incubator for *in vitro* electromagnetic waves exposure of adherent cells in tissue culture plates. Typical cell incubators require specific conditions such as temperature of 37°C and humidity rate of 95 % which are challenging conditions for a RC. The chamber was characterized as an RC through an innovative experimental methodology based on the measurements of the S_{11} parameter of the emitting antenna. The proposed RC is adapted for *in vitro* bioelectromagnetic experiments for simultaneous exposure of up to ten tissue culture plates under highly homogeneous exposure conditions at 3.5 GHz, i.e., the mid-frequency band of the 5G telecommunication networks. Results showed that the specific absorption rate (SAR) in the exposed samples extracted from temperature measurements was similar (an acceptable maximum variation lower than 30% was observed) in reason of the homogeneity and the uniformity of the field within the chamber. Specifically, measured SAR values were around 1.5 and 1 W/kg per 1 W of incident power, in 6-well or 96-well tissue culture plates used for biological exposure, respectively.

Index Terms—5G, cell culture incubator, *in vitro* exposure, mode stirrer, reverberation chamber, specific absorption rate (SAR), well stirred condition.

R. Orlacchio, G. Andrieu, and P. Leveque are with the University of Limoges, CNRS, XLIM, UMR 7252, F-87000 Limoges, France (e-mail: rosa.orlacchio@unilim.fr; guillaume.andrieu@unilim.fr; philippe.leveque@unilim.fr).

A. Joushomme, L. Patrignoni, A. Hurtier, F. Poulletier De Gannes, I. Lagroye, and Y. Percherancier are with the University of Bordeaux I, CNRS, IMS, UMR 5218 33400 Talence, France (e-mail: alexandre.joushomme@u-bordeaux.fr, lorenza.patrignoni@u-bordeaux.fr, annabelle.hurtier@ims-bordeaux.fr, florence.poulletier@ims-bordeaux.fr, isabelle.lagroye@ephe.psl.eu, yann.percherancier@ims-bordeaux.fr).

D. Arnaud-Cormos is with the University of Limoges, CNRS, XLIM, UMR 7252, F-87000 Limoges, France, and also with the Institut Universitaire de France (IUF), 75005 Paris, France (e-mail: delia.arnaud-cormos@xlim.fr).

I. INTRODUCTION

THE fifth generation of telecommunication technologies, i.e., the 5G, has been recently deployed to face the tremendous increase of mobile data traffic [1]. Numerous advantages are related to the use of 5G including faster data rates beyond several Gbit/s, low latency, more compact size of radiating structures, and lower interferences between devices [2]. The roll-out of 5G communication systems aims to improve the current mobile phone telecommunications in order to reach the ambitious project of an all-digital and hyper-connected society. The 5G technology will be indeed associated with the exponential growth of the Internet of Things (IoT) including, for instance, virtual reality, driverless cars, smart homes and cities, telemedicine [3]–[5].

In addition to the frequencies already used by existing generations of mobile telephony, three novel frequency bands will be exploited: the 700 MHz (694–790 MHz) and 3.5 GHz (3.4–3.8 GHz) bands and later on the 26 GHz band (24.25–27.5 GHz) [6]. Overall, such technological developments will impact general public exposure arising new questions about the safety and specific health effects of 5G. The majority of the already published studies, periodically reviewed over the last 30 years by international expert committees [7]–[10], concern the potential effects induced by 0.8–2.3 GHz and Wi-Fi signals at 2.45 GHz or higher frequencies around the 26, 40, and 60 GHz bands [11], [12]. However, existing scientific literature concerning the 3.5 GHz frequency band is rather limited (a complete review can be found in [6]). Thus, reported data is not sufficient to assess any established health effect deriving from these exposure levels [6], [13].

From a physical point of view, the electromagnetic (EM) characteristics of biological tissues absorption at 3.5 GHz are similar to those at frequencies between 1 and 2.5 GHz. To determine possible differences in terms of induced effects between the above-mentioned frequency bands, specific dosimetry studies and experimental evidence are required. To this end, new exposure setups able to precisely reproduce exposure conditions at 3.5 GHz must be designed.

Numerous exposure systems were developed over the years for bioelectromagnetic studies to assure reliable and reproducible exposure conditions for both *in vivo* and *in vitro*

studies [14]. Reverberation chambers (RCs) emerged, among others, as excellent instruments to enable longtime samples exposures to a homogeneous EM field [15]–[18].

RCs are electrically large enclosures with highly conductive walls where a statistically homogeneous, randomly polarized, and isotropic field distribution is achieved by mechanical or frequency stirring [19]. RCs were firstly proposed by the pioneer works of A. Mendez [20], P. Corona [21], and the National Institute of Standards and Technology (NIST) [22] to perform EM compatibility measurements. Nowadays, RCs are exploited by many applications for military activities [23], automobile industry [24], aeronautics [25], or the study of EM waves biological effects [26]. The possibility to use RCs for bioelectromagnetic applications was explored under the National Toxicology Program (NTP) for the simultaneous exposure of more than hundred unrestrained rodents individually housed in plastic cages up to 24 hours per day to Global System for Mobile Communications (GSM) and Code-Division Multiple Access (CDMA) at 0.9 and 1.9 GHz [16], [26], [27]. Compared to other exposure systems, RCs allow performing long time exposure with unrestrained animals while maintaining a high level of overall exposure efficiency. Therefore, RCs found increasing interest among the bioelectromagnetic society for the development of *in vivo* exposure systems operating within the 0.9–2.45 GHz band [16], [17], [26], [28]–[30]. In addition, RCs feasibility was also proved at frequencies as high as 10 GHz [31] or 60 GHz [32], [33]. To the best of our knowledge, *in vitro* exposures in an RC were only explored in [17]. Authors exposed up to eight petri dishes to 0.9 GHz frequency signal in a customized chamber able to provide the desired cellular conditions. A heating device and an air fan (located above and below the exposed samples, respectively) were used to maintain the chamber at 37°C while each dish was enclosed in a plexiglass box to control the desired level of CO_2 (5%). A low level of specific absorption rate (SAR) of the order of only few mW/kg was locally measured in the exposed dishes.

In this study, we propose a cell culture incubator converted into an RC adapted for *in vitro* exposure of several tissue culture plates (TCPs) at 3.5 GHz. 5G technology exposures can be achieved with this RC setup under a controlled atmosphere (37 °C, 5% CO_2). The proposed chamber was validated through EM and thermal measurements. The chamber was characterized in the 1–6 GHz frequency band using an innovative technique based on the measurements of the reflection coefficient of the emitting antenna. Then, local SAR was experimentally quantified at 3.5 GHz in the exposed cell culture medium.

The paper is organized as follows. The exposure system is presented in Section II and characterized in Section III. In Section IV, experimental results in terms of SAR are presented and discussed in detail. Conclusions are drawn in section V.

II. PRESENTATION OF THE EXPOSURE SYSTEM

The exposure system designed and characterized in this study is presented in Fig. 1. A BINDER CB 150 biological incubator (BINDER Gmbh, Tullingen, Germany), with stainless steel walls and inner dimensions of $0.5 \times 0.5 \times 0.6$ m, was used as a RC to guarantee a controlled atmosphere (37°C, 5% CO_2) during exposure of cells.

As illustrated in the inset of Fig. 1, a homemade patch antenna matched over the 1–6 GHz frequency range was used to deliver a continuous (CW) signal at 3.5 GHz into the RC. The antenna input was connected through an SMA cable to the signal generation unit located outside the incubator. The generation unit was composed of a radiofrequency (RF) signal generator (SMBV100A, Rohde & Schwarz, Munich) connected to a 45-dB gain, amplifier (Mini-circuits, ZHL-16W-43+, NY, USA) followed by a high-power circulator (Pasternack, PE83CR1005, CA, USA), and a bidirectional coupler (Mini-circuits, ZGBDC30-372HP+, NY, USA) connected to the antenna. Incident and reflected powers at the input of the antenna measured with two power sensors (Agilent N1921A, USA) were monitored with a power meter (Agilent N1912A, USA) connected to the bidirectional coupler.

As explained later, during SAR measurements, mechanical mode stirring process was used to continuously modify the boundary conditions of the whole system and therefore obtain an averaged homogeneous and isotropic EM field within the chamber [34]. A metallic stirrer composed of 8 rectangular blades of $8 \times 10 \times 1$ cm^3 was used (inset of Fig. 1). To allow continuous rotation of the stirrer during the exposure, a motorized precision rotation stage (PRM1/MZ8, Thorlabs Inc., Newton, NJ) driven via a K-Cube DC servo controller (KDC101, Thorlabs) was employed. Five plastic racks (209 $\times$ 172 $\times$ 62 mm^3, Dutscher, France) were piled up to obtain a compact structure accommodating up to ten TCPs (two per level). A 3-cm diameter hole on the incubator side allows connecting the antenna to the bidirectional coupler and the motor stage to the motor controller located outside the incubator. To ensure statistical field uniformity and isotropy, the antenna, the stirrer, and the plastic support were set in the chamber at a distance from each other greater than $\lambda/4$ and greater than $\lambda/2$ from the incubator walls, with λ being the wavelength at 3.5 GHz (e.g., 8.5 cm) [35].

A water reservoir, filled with 300 ml of water, located at the bottom of the chamber allowed maintaining the desired level of humidity (95%). A metallic grid located above the reservoir sustained the patch antenna, the metallic stirrer with its rotation stage, and the plastic support hosting the TCPs during the exposure. A homemade software allowed to monitor different parameters including the input power, the duration of the exposure, and the stirrer rotation.
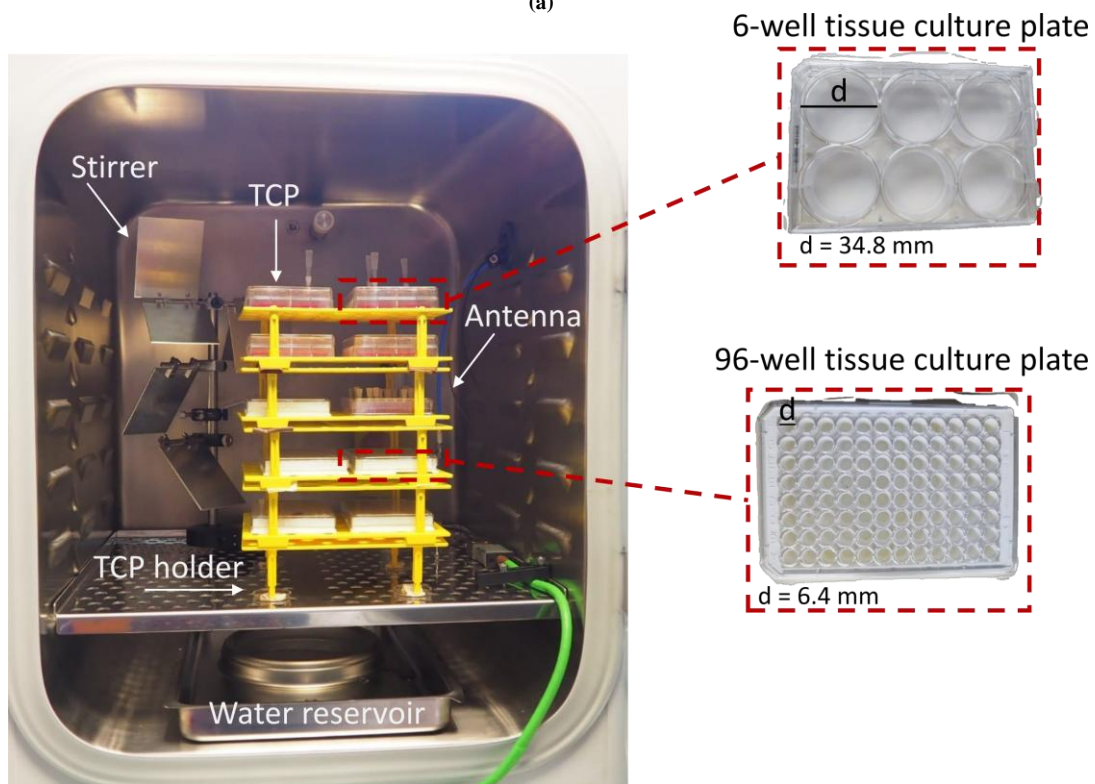
III. CHARACTERIZATION OF THE EXPOSURE SYSTEM AS AN RC

The performances of the exposure system as an RC must be characterized before application for *in vitro* bioelectromagnetic

experiments. To attain this objective, we have used the
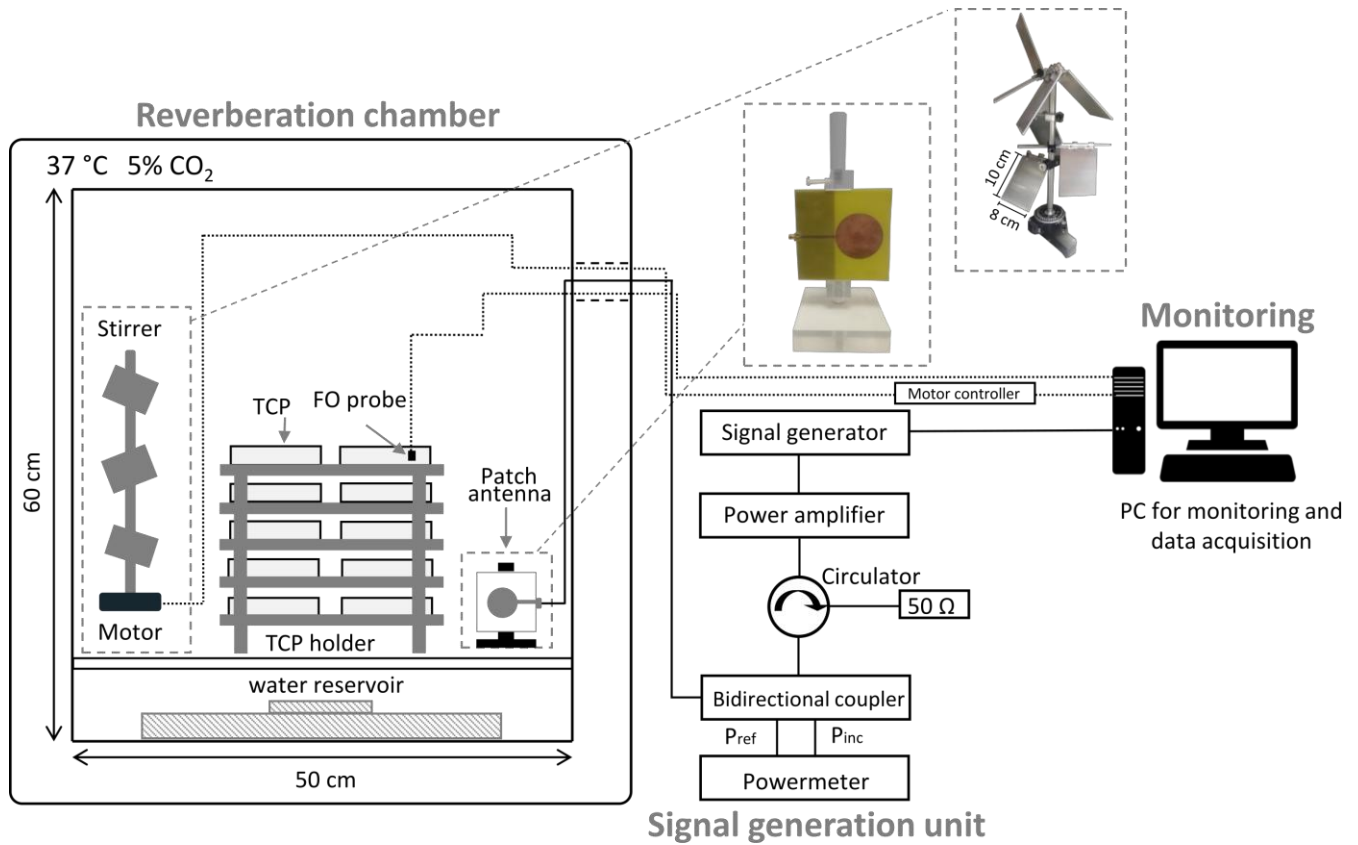
Fig. 1. **(a)** Schematic of the exposure system: 1) A cell culture incubator converted into a reverberation chamber containing the patch antenna, the stirrer with its motor, the plastic holder hosting ten tissue culture plates (TCPs), the fiber optic (FO) probe used for temperature measurements, and the water reservoir (*on the left*); 2) signal generation unit (*center*); 3) monitoring unit (*on the right*). Dimensions are not to scale. **(b)** Picture of the incubator containing the stirrer, the water reservoir, the antenna (on the back), and the holder of the TCPs. The insets on the right show a picture of a 6- (on the top) and 96- (on the bottom) well TCPs with diameter (d) of 34.8 and 6.4 mm, respectively, used in this study.
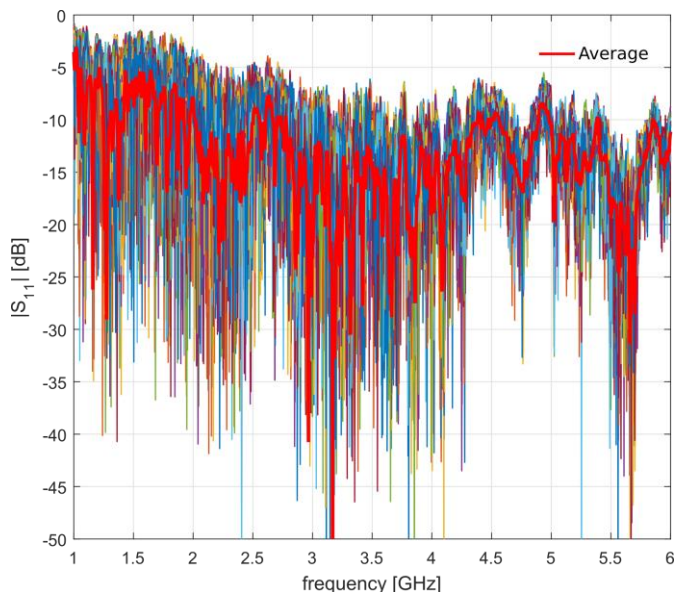
Fig. 2.   Magnitude of the S_{11} parameter of the antenna for the unloaded configuration of the exposure system measured over 50 positions of the mode stirrer (step = 7.2°). The red plot is the average value calculated over all the positions.

This method recently published [36], [37]. This method, briefly summarized hereafter, allows to determine the minimum operating frequency, defined as f_{wsc}, from which the chamber is considered "well-stirred" (WS). The exposure system was characterized from stepwise mode stirrer positions through measurements of the reflection coefficient, i.e., the S_{11} parameter of the emitting antenna.

A.   Well-Stirred Condition Method

The WS condition method investigates the ability of the chamber to produce an EM field matching the characteristics of a "well-stirred" (or ideal) RC. The complete definition of the WS method, given in [37], requires assessing, at a given frequency, the distribution of the EM field as well as the correlation of the collected samples. This is respectively carried out thanks to the Anderson-Darling (AD) goodness-of-fit (GOF) test [38] and to the first-order autocorrelation coefficient r(1) [39]. These parameters are extracted from the stirred part of the S_{11} parameter of the emitting antenna installed in the RC, calculated for each stirrer position through the removal of the S_{11} vector average obtained for the different stirrer positions. A polynomial curve fitting allows the definition of two different frequencies: f_1 related to the EM field distributions and f_2 related to the EM sample correlation. These frequencies are obtained using theoretically justified threshold values when each criterion corresponding to a WS RC is assumed to be respected. To ensure that both criteria are matched, the maximum value between f_1 and f_2 is considered as the f_{wsc} frequency. In this study, the S_{11} parameter of the emitting antenna, shown in Fig. 2., was measured with a vector network analyzer. Measurements were performed for N equal to 50 equidistant positions of the mode stirrer, with 7.2° between two

successive positions, over 1601 frequencies linearly spaced between 1 and 6 GHz. On the contrary, SAR measurements were performed with the stirrer continuously rotating during sample exposure.

The influence of the TCPs number introduced in the exposure system on f_1, f_2, and f_{wsc} was analyzed by progressively adding up to ten TCPs to the "unloaded" configuration of the incubator, i.e., the incubator containing the patch antenna, the stirrer and its motor stage, the reservoir with 300 ml of water and the support without TCPs.

To satisfy biological requirements, two types of TCPs with 6- and 96-well TCPs were used (inset of Fig. 1(b)). To guarantee a typical biological environment during exposure, each well of the 6- and 96- TCPs was respectively filled with 2 ml and 200 µl of cell culture medium (Dulbecco's modified Eagle medium, Gibco/Life Technologies, Carlsbad, CA).

The chamber was progressively loaded with the following configurations:

- 2 TCPs: two 6-well TCPs corresponding to 24 ml of cell culture medium;
- 4 TCPs: four 6-well TCPs (48 ml);
- 6 TCPs: four 6-well TCPs and two 96-well TCPs (86.4 ml);
- 8 TCPs: four 6-well TCPs and four 96-well TCPs (124.8 ml);
- 10 TCPs: four 6-well TCPs and six 96-well TCPs (163.2 ml).

Fig. 3 presents the results obtained for the unloaded configuration while Table I contains f_1, f_2, and f_{wsc} values for all the tested configurations. As observed, f_1 is always around 1 GHz signifying that the ideal EM field distributions (i.e., the Rayleigh distribution for the S_{11} stirred samples) are matched above this frequency for all the configurations. The slight variation of f_1 around 1 GHz, assumed not significant, is due to the sensitivity of the AD GOF test (see [36], [37] for further details). Moreover, the insertion of the TCPs in the RC induces as expected an increase of f_2, i.e., an increase of the correlation between the mode stirrer positions. Indeed, the frequency f_{wsc} varies from 3.3 to 4.5 GHz depending on the number of inserted TCPs in the exposure system. The addition of TCPs contributes to the decrease of the RC quality factor (Q-factor) which is known to increase the correlation of the measured samples.

It is worth noting that a value of f_{wsc} greater than 3.5 GHz (meaning that two successive mode stirrer positions are not perfectly uncorrelated at such frequency) still remains compliant, as shown later, with bioelectromagnetic exposures at this frequency. In particular, the fact that the ideal EM distributions of a well-stirred RC are well respected for frequencies above 1 GHz in all configurations allows to be confident on the homogeneity of the SAR values obtained at any location of the wells within the cell culture incubator (and this is demonstrated later in section IV).

B.   Quality Factor

The composite Q-factor of an RC is used to describe the ability of the chamber to store energy or in other terms the amount of losses occurring in the RC. For the RC
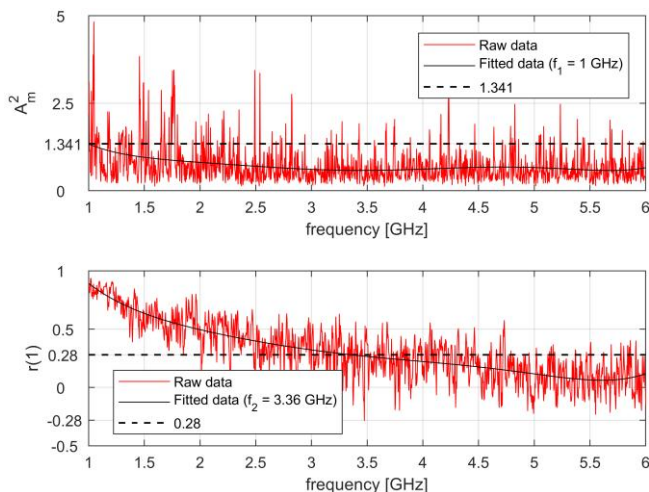
Fig. 3. Results related to the "well-stirred condition" method for the unloaded configuration of the exposure system. On the upper subplot, the corrected statistic A_m^2 of the AD GOF test for each frequency, the 6th order polynomial curve fit as well as the value of f_1 are presented. On the lower subplot, the first-order autocorrelation coefficient r(1) for each frequency, the 6th order polynomial curve fit as well as the value of f_2 are presented.

TABLE I
F_1, F_2, AND F_{WSC}, OF THE UNLOADED AND LOADED INCUBATOR WITH INCREASING NUMBER OF TISSUE CULTURE PLATES (TCPS)

Number of TCPs	Liquid volume (ml)	$f_{1\ (GHz)}$	$f_{2\ (GHz)}$	$f_{wsc\ (GHz)}$
0 (Unloaded)	0	< 1	3.36	3.36
2	24	< 1	3.62	3.62
4	48	1.09	3.82	3.82
6	86.4	1.06	4.22	4.22
8	124.8	1.08	4.3	4.3
10	163.2	1.15	4.5	4.5

characterization process, establishing the Q-factor parameter is fundamental. The Q-factor is defined as the ratio between mean stored and transmitted energies in the chamber [40]:

$$Q = \frac{\omega\varepsilon\langle|E^2|\rangle V}{P_t} \qquad (1)$$

with ω the angular frequency (rad/s), ε the permittivity (F/m), V the RC volume (m^3), $\langle|E|\rangle$ the average total electric field strength (V/m), and P_t the antenna transmitted power (W).

The Q-factor can be experimentally estimated from the S_{11} measurement of an antenna [40]:

$$Q = \langle|S_{11} - \langle S_{11}\rangle|^2\rangle \frac{Z_0\omega\varepsilon V}{\left(\lambda^2/(4\pi)\right)(1 - |\langle S_{11}\rangle|^2)^2\eta^2} \qquad (2)$$

with ω the angular frequency (rad/s), ε the permittivity (F/m), V the RC volume (m^3), Z_0 the wave impedance (Ω), η the antenna efficiency, and λ the wavelength (m).

The estimated Q obtained from S_{11} measurements over the whole frequency band considered in this study for three different loading configurations is reported in Fig. 4. As observed, the Q-factor even in the unloaded configuration is relatively low (lower than 1000). This is also consistent with the EM field distributions which are verified above 1 GHz due
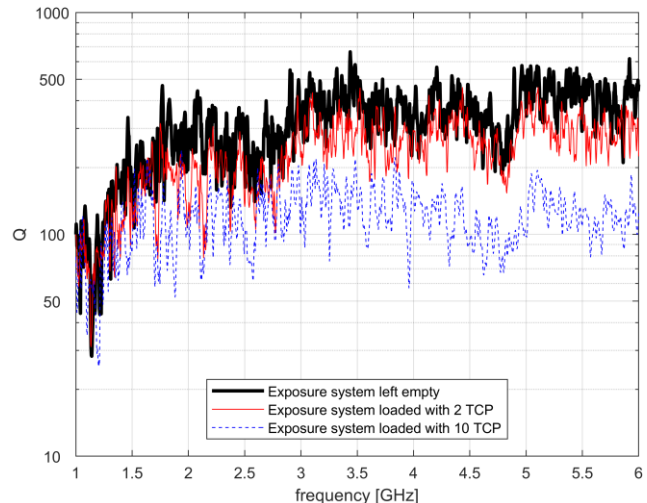

Fig. 4. Comparison of the average quality factor (Q) of the exposure system calculated using (2) for 3 different configurations, including the unloaded incubator, or loaded with 2 and 10 tissue culture plates (TCP).

to the excellent modal recovering [41] and also with the residual correlation observed at 3.5 GHz. As expected, the insertion of 2 TCPs results in a greater Q-factor ($\sim$ 280) compared to 10 TCPs ($\sim$ 135) around the frequency of 3.5 GHz (values averaged over a 40 MHz bandwidth).

In addition, the knowledge of Q allows predicting the average total electric field $\langle|E|\rangle$, which can be obtained in the RC for a given transmitted power P_t [36]:

$$\langle|E|\rangle = \sqrt{\frac{QP_t}{\omega\varepsilon V}}\frac{15}{16}\sqrt{\frac{\pi}{3}} \qquad (3)$$

Therefore, for 13 W of incident power, the estimated E-field in the incubator at 3.5 GHz is between approximatively 360 and 250 V/m when varying the load from 2 to 10 TCPs, respectively.

IV? *Numerical Simulations*

To validate experimental dosimetry, numerical simulations were also performed using a three-dimensional finite difference time domain (FDTD)-based electromagnetic method [42]–[44]. This allows the investigation of SAR values and homogeneity within the exposed samples.

Computer- aided design (CAD) model of the exposure system is represented in Fig. x. The cell culture incubator was modelled as a metallic box of x × x × x m^3. All the elements inside the chamber were modelled, including the patch antenna, the stirrer (motor?), the water reservoir, and the plastic support accommodating 10 TCPs. The patch antenna was modeled as… Stirrer…

The TCP and the support were modeled as polystyrene with a relative permittivity ε_r and an electrical conductivity σ (S/m) of x and x S/m, respectively. For the cell culture medium, at 3.5 GHz, ε_r and σ (S/m) of x and x were used, respectively.

The simulations were performed using a mesh with a cell size ranging from x µm in the liquid up to y µm in free space. XXX boundary conditions were used.

Fig. 6. 6-well tissue culture plate used for exposure. Temperature measurements were performed i) in the center of each well at the location indicated by the number 1, and ii) at different locations in well number 4 indicated by the numbers from 1 to 5. Distance of points 2 to 5 from point 1 (a) equals to ~1.5 cm, while distance from the well edge (b) equals to ~ 2 mm.

rotation of the stirrer with 7.2° between two successive positions, and averaged to obtain SAR values…

IV. RESULTS

In this section, SAR values retrieved through experimental measurements are presented and discussed.

A. SAR Measurements Protocol

SAR is defined as the EM power dissipated per unit mass in the exposed sample and it represents the basic dosimetric parameter used to quantify the exposure levels at a given frequency. SAR can be obtained either from the measurement of the EM-induced heating or from electric field values in the medium [42]. Herein, temperature measurements during exposure were performed in cell culture medium (Dulbecco's modified eagle medium [Gibco/Life Technologies, Carlsbad, CA]) to retrieve local SAR values from the initial phase of the heating kinetics using the following equation:

$$SAR = C \left.\frac{\partial T}{\partial t}\right|_{t=t_0} \tag{4}$$

where C is the biological sample heat capacity (typically 4180 J/(kg·K) for cell culture medium) and $\partial T/\partial t$ is the initial slope of the temperature curve when the effect of thermal convection on the exposed liquid is negligible [43].

A fiber-optic (FO) thermometer (Luxtron One, Lumasense Technologies, CA, USA) was used in our experiments to acquire local temperature elevation within an estimated 1 mm^3 volume inside the exposed medium. Samples were exposed during 144-s with the mode stirrer continuously rotating at a constant angular velocity of 10 degrees per second, i.e., four complete revolutions of the stirrer. Measurements were performed under continuous wave signal at 3.5 GHz for an antenna input power of 13 W all along the exposure cycle and repeated at least n = 3 times per each condition in order to assess repeatability.

B. Results

1) SAR Measurements Uncertainty

SAR values fitted from the initial phase of the temperature dynamics highly depends on the curve noise of the acquisition
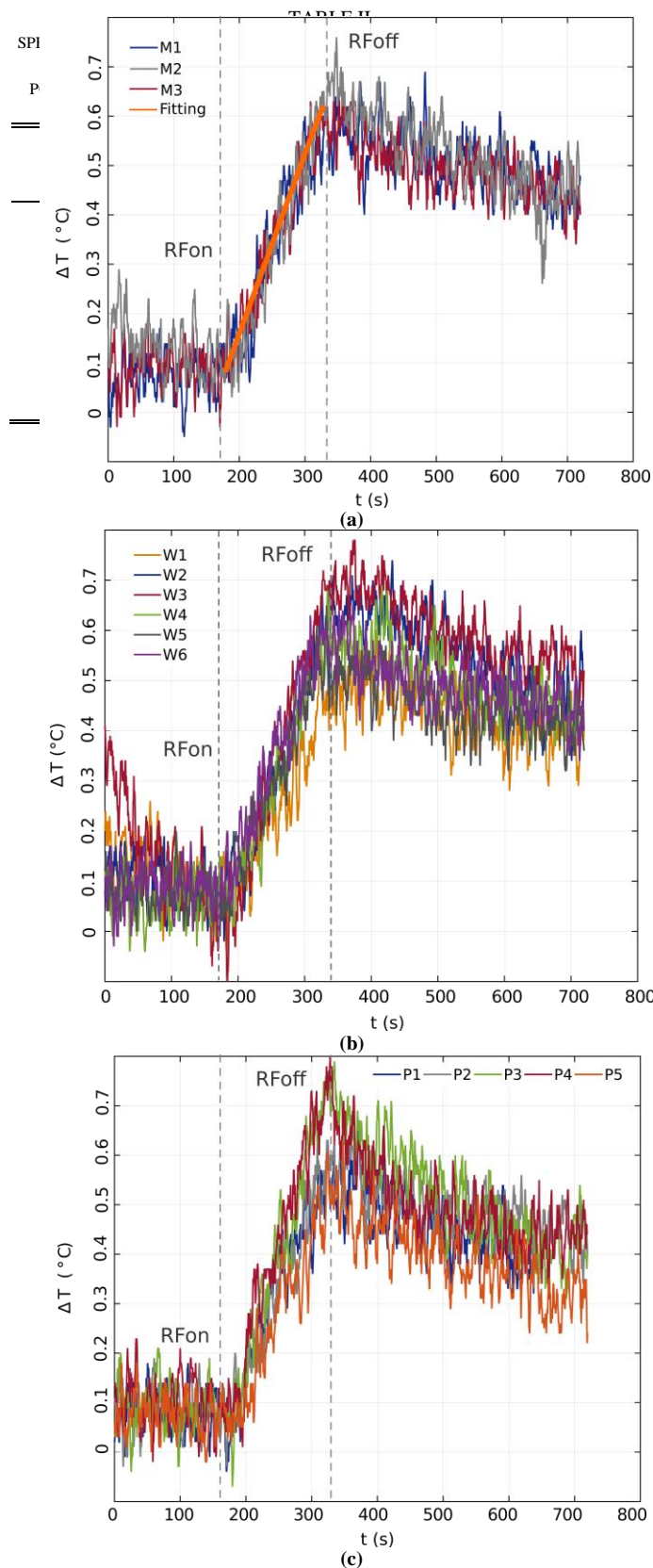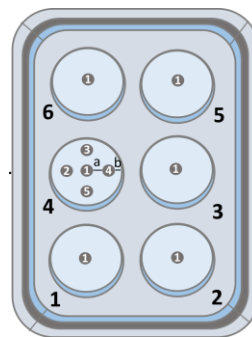
Fig. 5. Temperature elevation measured during exposure in 6-well tissue culture plates (TCPs) during 144-s of exposure at 13 W of incident power for the incubator loaded with 10 TCPs. Reproducibility is shown for measurements performed in (a) point #1 of the same well (n=3), (b) point #1 of 6 wells of a TCP, and (c) points from #1 to #5 of the same well. Orange line in (a) indicates the fitting curve used to retrieve local SAR. Grey dashed lines indicate the beginning (RFon) and the end (RFoff) of the radiofrequency (RF) exposure. Location of points (#1 to #5) and wells is indicated in Fig. 6.

system. In this study, induced temperature elevation was exponentially fitted along the whole exposure duration, i.e., 144 s from RF ON to RF OFF (Figs. 5,7-8). However, only the slope at the origin was considered for SAR calculation using (4).

Fig. 5(a) shows three independent temperature measurements, i.e., temperature rise recorded at different moments in the center of the same well (point #1 of Fig. 6). ΔT (°C) represents the temperature variation of the liquid with respect to the temperature before exposure, i.e., between RF ON and RF OFF in Figs. 5,7-8. Temperature curves are highly reproducible at the same probe location and a 10% uncertainty on the local SAR is observed, mostly due to the noise of the acquired temperature rise.

2) SAR Values in the 6-Well TCP

Local SAR of the 6-well TCP (Fig. 6) was measured in the wells of the two TCPs (left and right positions) located on the top of the holder. In this case, measurements were performed with the chamber loaded under the requested conditions for biological experiments, i.e., 10 TCPs. Homogeneity of SAR within all the exposed wells was confirmed by measurements in several wells at different TCPs locations on the holder levels.

To assess SAR homogeneity, measurements were performed: i) in the center of each of the six wells of the TCP (points #1 of Fig. 6), and ii) in 5 positions within the same well (points from #1 to #5 in well number 4 of Fig. 6). Fig. 5(b) and Fig. 5(c) reporting the corresponding results, shows a high reproducibility of the measurements. SAR values extrapolated from the first phase of the heating kinetics in six different wells

or in the same well are reported in Tables II and III, respectively (n = 3 for each location). Average local SARs in the center of the wells (points #1), obtained by pooling all recorded data of the plate in the six wells (n = 18, i.e., 3 measurements × 6 wells) for the left and right TCP were 1.49 ± 0.17 and 1.42 ± 0.11 W/kg/P_{inc}, respectively. Local SAR values measured in each well are reported in Table II. These results show high reproducibility at the same point and good homogeneity between the wells with a standard deviation within 15% suggesting that measurements are independent of the position within the chamber.

Global average SAR values of a single well with a diameter of 34.8 mm were obtained by pooling all recorded data in the same well at different locations (n = 15, 3 measurements × 5 positions). The SAR values were 1.56 ± 0.36 and 1.61 ±

TABLE III
SPECIFIC ABSORPTION RATE (SAR) VALUES EXTRAPOLATED IN 5 POINTS OF THE SAME WELL OF TWO 6-WELL TISSUE CULTURE PLATES (LEFT AND RIGHT POSITIONS ON THE TOP OF THE HOLDER). DATA ARE PRESENTED AS MEAN ± STANDARD DEVIATION (N = 3)

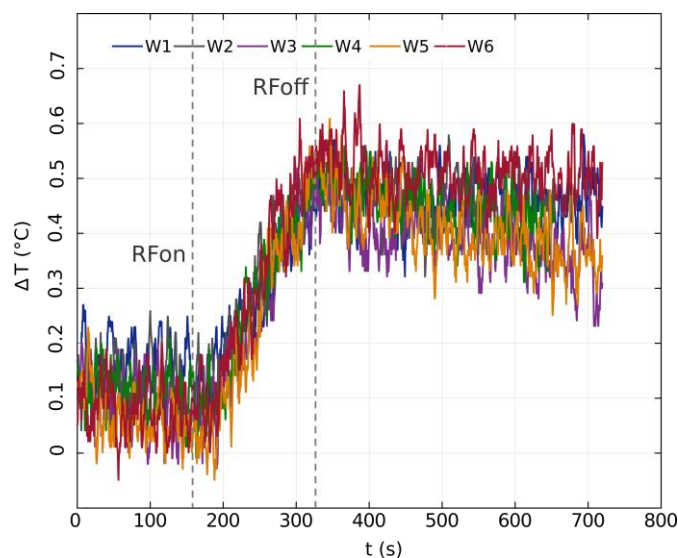| Position	Left	Right
	SAR (W/kg/P_{inc})	
1	1.36 ± 0.14	1.37 ± 0.12
2	1.03 ± 0.26	1.22 ± 0.12
3	1.86 ± 0.09	1.74 ± 0.21
4	1.87 ± 0.01	2.06 ± 0.05
5	1.71 ± 0.17	1.7 ± 0.09

Fig. 7. Temperature elevation measured in 6 wells of a 96-well tissue culture plate during 144-s of exposure at 13 W of incident power for the incubator loaded with 10 TCPs. The grey dashed lines indicate the beginning (RFon) and the end (RFoff) of the radiofrequency (RF) exposure.

0.33 W/kg/P_{inc} for the well on the left and right side of the support, respectively. Maximal variation of SAR observed between the different positions considered in the well was within 30% (Table III). The larger variation of the results in this case corresponds also probably to the fact that the probe is not
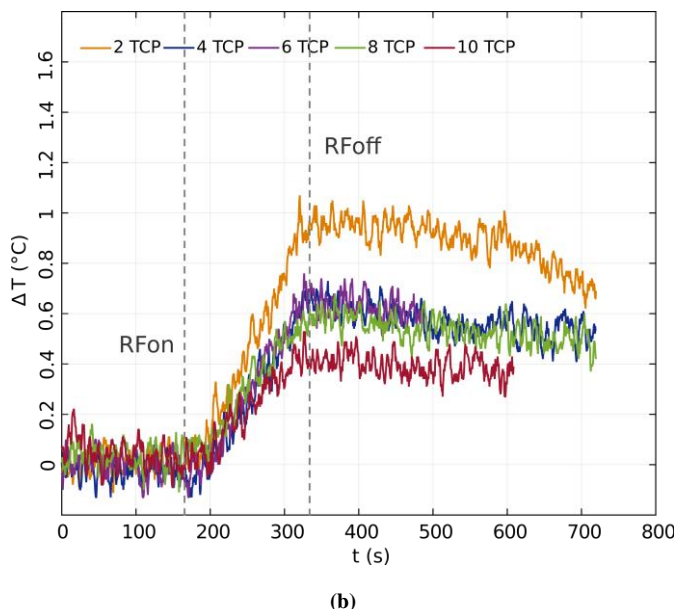

(a)

(b)
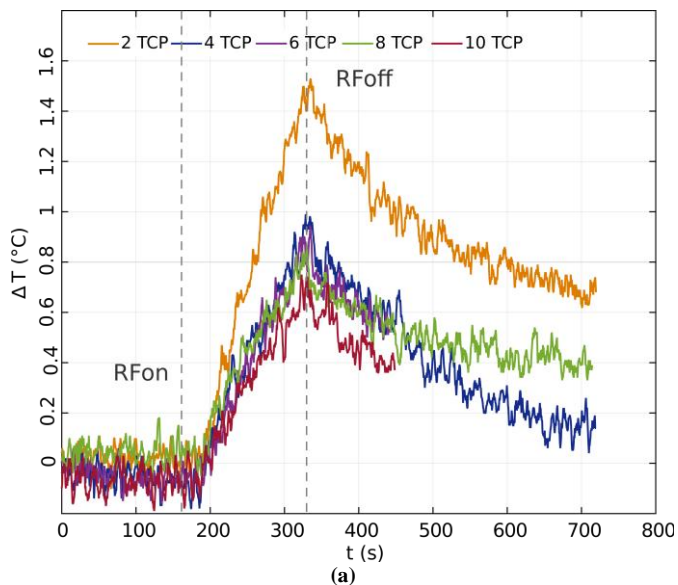
Fig. 8. Temperature elevation during 144-s of exposure at 13 W of incident power for different incubator loads from 2 to 10 tissue culture plates (TCPs) for (a) 6- well and (b) 96- well TCP. The grey dashed lines indicate the beginning (RFon) and the end (RFoff) of the radiofrequency (RF) exposure.

TABLE IV
SPECIFIC ABSORPTION RATE (SAR) VALUES AS A FUNCTION OF THE CHAMBER LOADING IN 6-AND 96-WELL TISSUE CULTURE PLATES (TCPs). DATA ARE PRESENTED AS MEAN ± STANDARD DEVIATION (N = 3)

	Number of TCPs				
	2	4	6	8	10
	SAR (W/kg/P_{inc})				
6-well	2.91±0.05	2.13±0.54	2.14±0.17	1.93±0.06	1.8±0.31
96-well	2.56±0.06	1.62±0.19	1.75±0.07	1.24±0.2	1.1±0.07

centered in the middle of the cell in positions #2 to #5. Note that the effect of the meniscus at the interface between the liquid and the plastic walls can significantly impact SAR distribution [44], [45]. However, this variation is compliant with values defined by international standards for EM waves exposures within the 300 MHz – 300 GHz band [46].

3) SAR Values in the 96-Well TCP

SAR was also evaluated in 16 different wells of the 96-well TCPs located on the top left and right side of the support. An example of the temperature dynamics recorded is reported in Fig. 7. In this case, due to the small diameter of the well (6.4 mm), one probe location was measured per each well. SAR was equal to 1.07 ± 0.25 and 0.91 ± 0.3 W/kg/P_{inc} in the left and right

plates, respectively (n = 16). SAR values are also within a standard deviation of about 30%.

4) SAR Values as a Function of the Incubator Loading

Experimental SAR was retrieved in both 6- and 96-well TCPs as a function of the chamber loading (n = 3 measurements per loading condition). Fig. 8 shows the temperature elevation induced in the center of one well of the exposed TCP (6- or 96-well) set on the top of the holder as a function of the incubator loading.

When two TCPs are used, temperature elevation and corresponding induced SAR are higher compared to the other loading conditions. Loading the chamber from 2 to 10 TCPs introduces a non-linear SAR decrease of 38% and 57% for the 6-and 96-well TCPs, respectively (Table IV). This is due to the smaller liquid volume contained in the chamber loaded with 2 TCPs (SAR is defined as the power absorption per unit mass) thus higher Q-factor and E-field levels. Indeed, considering that SAR is proportional to $|E|^2$ [42], an higher E-field implies an higher SAR.

V. CONCLUSION

In this study, we have designed and characterized the first cell culture incubator developed as an RC for *in vitro* exposure of multiple TCPs in the mid band of the 5G telecommunication networks. The chamber is designed to host up to 10 TCPs under controlled conditions, 37°C and 5% CO_2, allowing homogeneous EM exposure within the same type of TCP up to 24 hours. Mechanical stirring of the EM exposure emitted by a printed antenna was achieved with eight 8×10 cm² metallic blades mounted on a mast continuously rotating during exposure.

The RC was first experimentally characterized through measurements of the scattering parameter S_{11} of the antenna using a fast methodology. We showed that increasing the chamber loading increases the f_{wsc} which was equal to 3.36 GHz and 4.5 GHz for the unloaded and loaded chamber with 10 TCPs, respectively. This is due to the increase of the correlation of the stirrer positions. Consistently, the experimental Q-factor assessed at 3.5 GHz decreases due to losses in the chamber from values of approximatively 316 to 135, when the incubator was unloaded or loaded with 10 TCPs, respectively.

SAR values were then assessed through measurements of the EM-induced temperature elevation in the samples exposed to 3.5 GHz. Mean SAR levels in the 6-and 96-well TCPs were around 1.5 and 1 W/kg per watt antenna input power, respectively. These SAR values were obtained when the chamber was loaded with 10 TCPs and they were independent of the wells position in the chamber. Moreover, during exposure, the EM fields components were continuously stirred resulting in the achievement of SAR homogeneity with maximal variations lower than 30%. All the results presented in the paper prove the relevance of our approach aiming to convert a cell culture incubator into an RC. Despite the relative low Q-factor of the facility, the obtained results show a remarkable homogeneity of the results as a function of the position of the wells within the enclosure. This homogeneity is assumed to be related to the characteristics of the RC really close to be perfectly well-stirred at the frequency of 3.5 GHz. Therefore, the exposure system reported in this paper leads the way towards the study at cellular and molecular levels of 3.5 GHz 5G exposures.

REFERENCES

[1] J. Navarro-Ortiz, P. Romero-Diaz, S. Sendra, P. Ameigeiras, J. J. Ramos-Munoz, and J. M. Lopez-Soler, "A Survey on 5G Usage Scenarios and Traffic Models," *IEEE Communications Surveys Tutorials*, vol. 22, no. 2, pp. 905–929, 2020, doi: 10.1109/COMST.2020.2971781.

[2] S. Kumar, A. S. Dixit, R. R. Malekar, H. D. Raut, and L. K. Shevada, "Fifth Generation Antennas: A Comprehensive Review of Design and Performance Enhancement Techniques," *IEEE Access*, vol. 8, pp. 163568–163593, 2020, doi: 10.1109/ACCESS.2020.3020952.

[3] J. Wang, M. K. Lim, C. Wang, and M.-L. Tseng, "The evolution of the Internet of Things (IoT) over the past 20 years," *Computers & Industrial Engineering*, vol. 155, p. 107174, May 2021, doi: 10.1016/j.cie.2021.107174.

[4] S. Li, L. D. Xu, and S. Zhao, "5G Internet of Things: A survey," *Journal of Industrial Information Integration*, vol. 10, pp. 1–9, Jun. 2018, doi: 10.1016/j.jii.2018.01.005.

[5] K. Shafique, B. A. Khawaja, F. Sabir, S. Qazi, and M. Mustaqim, "Internet of Things (IoT) for Next-Generation Smart Systems: A Review of Current Challenges, Future Trends and Prospects for Emerging 5G-IoT Scenarios," *IEEE Access*, vol. 8, pp. 23022–23040, 2020, doi: 10.1109/ACCESS.2020.2970118.

[6] ANSES- Agence nationale de sécurité sanitaire de l'alimentation, de l'environnement et du travail, "Expositions aux champs électromagnétiques liées au déploiement de la technologie de communication « 5G » et effets sanitaires éventuels associés." Apr. 2021.

[7] Strålsäkerhetsmyndigheten (Swedish Radiation Safety Authority), "2020:04 Recent research on EMF and health Risk," - *Fourteenth report from SSM's scientific council on electromagnetic fields*, Apr. 2020.

[8] Strålsäkerhetsmyndigheten (Swedish Radiation Safety Authority), "2019:08 Recent research on EMF and health risk," - *Thirteenth report from SSM's scientific council on electromagnetic fields*, Aug. 2018.

[9] ANSES- Agence nationale de sécurité sanitaire de l'alimentation, de l'environnement et du travail, "Expositions aux téléphones mobiles portés près du corps." 2019.

[10] SCENIHR (Scientific Committee on Emerging and Newly Identified Health Risks), "Opinion on potential health effects of exposure to electromagnetic fields (EMF)," Jan. 2015.

[11] M. Simkó and M.-O. Mattsson, "5G Wireless Communication and Health Effects—A Pragmatic Review Based on Available Studies Regarding 6 to 100 GHz," *Int J Environ Res Public Health*, vol. 16, no. 18, Sep. 2019, doi: 10.3390/ijerph16183406.

[12] Y. Le Drean *et al.*, "State of knowledge on biological effects at 40-60 GHz [Le point sur les effets biologiques à 40-60 GHz]," *Comptes Rendus*

Physique, vol. 14, no. 5, pp. 402–411, May 2013, doi: 10.1016/j.crhy.2013.02.005.

[13] A. Di Ciaula, "Towards 5G communication systems: Are there health implications?," *International Journal of Hygiene and Environmental Health*, vol. 221, no. 3, pp. 367–375, Apr. 2018, doi: 10.1016/j.ijheh.2018.01.011.

[14] J. W. Hansen *et al.*, "A Systematic Review of In Vitro and In Vivo Radio Frequency Exposure Methods," *IEEE Rev Biomed Eng*, vol. 13, pp. 340–351, 2020, doi: 10.1109/RBME.2019.2912023.

[15] K. B. Jung *et al.*, "Development and validation of reverberation-chamber type whole-body exposure system for mobile-phone frequency," *Electromagn Biol Med*, vol. 27, no. 1, pp. 73–82, 2008, doi: 10.1080/15368370701878895.

[16] M. H. Capstick *et al.*, "A Radio Frequency Radiation Exposure System for Rodents Based on Reverberation Chambers," *IEEE Trans. Electromagn. Compat.*, vol. 59, no. 4, pp. 1041–1052, Aug. 2017.

[17] S. Lalléchère, S. Girard, D. Roux, P. Bonnet, F. Paladian, and A. Vian, "Mode Stirred Reverberation Chamber (MSRC): a large and efficient tool to lead high frequency bioelectromagnetic in vitro experimentation," *Progress In Electromagnetics Research B*, vol. 26, pp. 257–290, 2010.

[18] J. Chakarothai, J. Wang, O. Fujiwara, K. Wake, and S. Watanabe, "Dosimetry of a Reverberation Chamber for Whole-Body Exposure of Small Animals," *IEEE Transactions on Microwave Theory and Techniques*, vol. 61, no. 9, pp. 3435–3445, 2013, doi: 10.1109/TMTT.2013.2273761.

[19] D. A. Hill, "Electromagnetic Theory of Reverberation Chambers," vol. 1506, Dec. 1998.

[20] Mendez, "A New Approach to Electromagnetic Field-strength Measurements in Shielded Enclosures".

[21] P. Corona, G. Latmiral, E. Paolini, and L. Piccioli, "Use of a Reverberating Enclosure for Measurements of Radiated Power in the Microwave Range," *IEEE Transactions on Electromagnetic Compatibility*, vol. EMC-18, no. 2, pp. 54–59, 1976, doi: 10.1109/TEMC.1976.303466.

[22] M. L. Crawford and G. Koepke, "Design, Evaluation and Use of a Reverberation Chamber for Performing Electromagnetic Susceptibility/VulnerabilityMeasurements," 1986.

[23] C. Choeysakul, F. Schlagenhaufer, P. Rattanakreep, and P. Hall, "EMC applications for military: Reverberation chamber tests," in *The 20th Asia-Pacific Conference on Communication (APCC2014)*, Pattaya, Thailand, Oct. 2014, pp. 434–437. doi: 10.1109/APCC.2014.7092851.

[24] Q. Xu, X. Shen, K. Chen, Y. Zhao, and Y. Huang, "Absorption cross section measurement of a vehicle in reverberation chamber for quick estimation of field strength," *IEEE Electromagnetic Compatibility Magazine*, vol. 8, no. 4, pp. 44–49, 2019, doi: 10.1109/MEMC.2019.8985598.

[25] D. M. Johnson, M. B. Slocum, and D. Hoskins, "High-power radiated susceptibility testing of rescue hoist systems in reverberation chambers," in *19th DASC. 19th Digital Avionics Systems Conference. Proceedings (Cat. No.00CH37126)*, Oct. 2000, vol. 1, p. 3B2/1-3B2/8 vol.1. doi: 10.1109/DASC.2000.886923.

[26] Y. Gong *et al.*, "Life-Time Dosimetric Assessment for Mice and Rats Exposed in Reverberation Chambers for the Two-Year NTP Cancer Bioassay Study on Cell Phone Radiation," *IEEE Transactions on Electromagnetic Compatibility*, vol. 59, no. 6, pp. 1798–1808, Dec. 2017, doi: 10.1109/TEMC.2017.2665039.

[27] National Toxicology Program (NTP), "NTP Technical Report on the Toxicology and Carcinogenesis Studies in B6C3F1/N Mice Exposed to Whole-Body Radio Frequency Radiation at a Frequency (1,900 MHz) and Modulations (GSM and CDMA) Used by Cell Phones," 596, Nov. 2018. doi: 10.22427/NTP-TR-596.

[28] T. Wu, A. Hadjem, M.-F. Wong, A. Gati, O. Picon, and J. Wiart, "Whole-body new-born and young rats\textquotesingle exposure assessment in a reverberating chamber operating at 2.4 GHz," *Phys. Med. Biol.*, vol. 55, no. 6, pp. 1619–1630, Feb. 2010, doi: 10.1088/0031-9155/55/6/006.

[29] P. F. Biagi *et al.*, "A Reverberation Chamber to Investigate the Possible Effects of," *Progress In Electromagnetics Research*, vol. 94, pp. 133–152, 2009, doi: 10.2528/PIER09061006.

[30] S. Jeon *et al.*, "Field Uniformity Assessment of a Reverberation Chamber for a Large-Scale Animal Study," *IEEE Access*, vol. 9, pp. 146471–146477, 2021.

[31] J. Shi, J. Chakarothai, J. Wang, O. Fujiwara, K. Wake, and S. Watanabe, "Improvement of SAR Accuracy by Combining Two SAR Quantification Methods for Small Animals in Reverberation Chamber Above 10 GHz," *IEEE Access*, vol. 8, pp. 138170–138178, 2020.

[32] A. K. Fall, P. Besnier, C. Lemoine, M. Zhadobov, and R. Sauleau, "Design and Experimental Validation of a Mode-Stirred Reverberation Chamber at Millimeter Waves," *IEEE Transactions on Electromagnetic Compatibility*, vol. 57, no. 1, pp. 12–21, février 2015, doi: 10.1109/TEMC.2014.2356712.

[33] A. K. Fall, C. Lemoine, P. Besnier, R. Sauleau, Y. L. Dréan, and M. Zhadobov, "Exposure Assessment in Millimeter-Wave Reverberation Chamber Using Murine Phantoms," *Bioelectromagnetics*, vol. 41, no. 2, p. 121, 2020.

[34] R. Serra *et al.*, "Reverberation chambers a la carte: An overview of the different mode-stirring techniques," *IEEE Electromagn. Compat. Mag.*, vol. 6, no. 1, pp. 63–78, 2017, doi: 10.1109/MEMC.2017.7931986.

[35] D. A. Hill, "Boundary fields in reverberation chambers," *IEEE Transactions on Electromagnetic Compatibility*, vol. 47, no. 2, pp. 281–290, May 2005, doi: 10.1109/TEMC.2005.847370.

[36] G. Andrieu, "Performance of reverberation chambers using the using the 'well-stirred condition method,'" *Electromagnetic Reverberation Chambers: Recent advances and innovative applications*, pp. 7–43, Dec. 2020.

[37] G. Andrieu, N. Ticaud, F. Lescoat, and L. Trougnou, "Fast and Accurate Assessment of the 'Well Stirred Condition' of a Reverberation Chamber From $_{11}$ Measurements," *IEEE Transactions on Electromagnetic Compatibility*, vol. 61, no. 4, pp. 974–982, Aug. 2019, doi: 10.1109/TEMC.2018.2847727.

[38] C. Lemoine, P. Besnier, and M. Drissi, "Investigation of Reverberation Chamber Measurements Through High-Power Goodness-of-Fit Tests," *IEEE Transactions on Electromagnetic Compatibility*, vol. 49, no. 4, pp. 745–755, 2007, doi: 10.1109/TEMC.2007.908290.

[39] O. Lunden and M. Backstrom, "Stirrer efficiency in FOA reverberation chambers. Evaluation of correlation coefficients and chi-squared tests," in *IEEE International Symposium on Electromagnetic Compatibility. Symposium Record (Cat. No.00CH37016)*, Aug. 2000, vol. 1, pp. 11–16 vol.1. doi: 10.1109/ISEMC.2000.875529.

[40] P. Besnier, C. Lemoine, and J. Sol, "Various estimations of composite Q-factor with antennas in a reverberation chamber," in *2015 IEEE International Symposium on Electromagnetic Compatibility (EMC)*, 2015, pp. 1223–1227. doi: 10.1109/ISEMC.2015.7256344.

[41] A. Adardour, G. Andrieu, and A. Reineix, "On the Low-Frequency Optimization of Reverberation Chambers," *IEEE Transactions on Electromagnetic Compatibility*, vol. 56, no. 2, pp. 266–275, Apr. 2014, doi: 10.1109/TEMC.2013.2288001.

[42] IEEE, "IEEE Recommended Practice for Determining the Peak Spatial-Average Specific Absorption Rate (SAR) in the Human Head from Wireless Communications Devices: Measurement Techniques," *IEEE Std 1528-2013 (Revision of IEEE Std 1528-2003)*, pp. 1–246, Sep. 2013.

[43] R. Orlacchio *et al.*, "Millimeter-Wave Heating in In Vitro Studies: Effect of Convection in Continuous and Pulse-Modulated Regimes," *Bioelectromagnetics*, vol. 40, no. 8, pp. 553–568, 2019, doi: https://doi.org/10.1002/bem.22223.

[44] J. Schuderer and N. Kuster, "Effect of the meniscus at the solid/liquid interface on the SAR distribution in Petri dishes and flasks," *Bioelectromagnetics*, vol. 24, no. 2, pp. 103–108, février 2003, doi: 10.1002/bem.10066.

[45] A. W. Guy, C. K. Chou, and J. A. McDougall, "A quarter century of in vitro research: a new look at exposure methods," *Bioelectromagnetics*, vol. Suppl 4, pp. 21–39, 1999, doi: 10.1002/(sici)1521-186x(1999)20:4+<21::aid-bem5>3.0.co;2-m.

[46] ICNIRP, "Guidelines for Limiting Exposure to Electromagnetic Fields (100 kHz to 300 GHz)," *Health Physics*, vol. 118, no. 5, pp. 483–524, May 2020, doi: 10.1097/HP.0000000000001210.
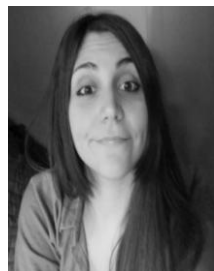
Rosa Orlacchio was born in Sapri, Italy. She received the M.Sc. degree in Biomedical Engineering, (with honors), from "La Sapienza", University of Rome, Roma, Italy, and the Ph.D. degree in Bio-electromagnetics from

the Institute of Electronics and Telecommunications of Rennes (IETR), University of Rennes 1, Rennes, France, in 2014 and 2019, respectively. She is currently a Postdoctoral Researcher with the BioEM Team, XLIM Research Institute, CNRS, University of Limoges, Limoges, France. Her current research interests include the evaluation of the biological effects of nanosecond electric pulses (nsPEF) on cells, and thermal electromagnetic dosimetry and microdosimetry.

Guillaume Andrieu (M'13–SM'17) was born in Limoges, France, in 1980. He received the master's degree in radiofrequencies and optical communications from the University of Limoges, Limoges, in 2003, and the Ph.D. degree in Electronics from the IEMN Laboratory, Telice Group, University of Lille, Villeneuve d'Ascq, France, in 2006. In 2003, he joined the Renault Technocentre, Guyancourt, France. In 2006, he joined the XLIM Laboratory, University of Limoges, as a Post-Doctoral Fellow, where he has been an Associate Professor since 2009. His current research interests include coupling on cables and electromagnetic compatibility testing including reverberation chambers and bulk current injection tests.

Alexandre Joushomme is a PhD student in Biochemistry. After obtaining his master's degree in Biochemistry and Molecular Biology at the University of Bordeaux in 2019, he chose to carry out his thesis at the IMS laboratory. He designs BRET probes allowing the study of the molecular mechanisms of cells in real time. Thanks to this technique, he is looking for non-thermal effects of RF EMF on the structural and functional modulation of proteins. He also uses techniques such as impedancemetry and holomicroscopy to study the impact of RF EMF on cell development and death or on the response of proteins and metabolic pathways to pharmacological compounds.

Lorenza Patrignoni was born in 1990 in Tolentino, Italy. She received the master's degree in Chemistry and Technology of Drugs in 2015 from the University of Perugia, Perugia, Italy. She is doing her Ph.D. program at the Ecole Pratique des Hautes Etudes (Paris, France), in collaboration with the IMS laboratory of Bordeaux where she is engaged in the study of biological effects of Radiofrequency on human cells.

Annabelle Hurtier is a Bordeaux INP biologist technician at the IMS laboratory. She is in charge of animal facility

and is a specialist in animal welfare.

Florence Poulletier de Gannes, Ph.D., is a CNRS research engineer at the IMS laboratory. Her research deals mainly with the adverse and beneficial biological effects of non-invasive electromagnetic fields funded by several national and foreign projects. She also works on EMF health risk assessment.

Isabelle Lagroye received the Master degree in 1991, the Pharm. D. degree and the Ph.D. degree in life science in 1997, from the Bordeaux 2 University, Bordeaux, France. After a Postdoctoral position at the Radiation Oncology Center, Dr. Roti-Roti's laboratory, Saint-Louis, MO, USA, she has been doing research work with the Bioelectromagnetics Team, IMS Laboratory, University of Bordeaux, Bordeaux, since 1999. She is a Professor at the Ecole Pratique des Hautes Etudes, Paris, France. Her main research interests include the toxicological effects of noninvasive electromagnetic fields, investigating genotoxicity, apoptosis, protein expression, and stress markers in rat brain and cell cultures exposed to mobile telephone signals. She earlier studied the effect of 50-Hz magnetic fields on cellular transformation and oncoproteins expression. She is an author of 40 peer-reviewed papers and more than 20 invited conferences and 50 conferences. She was a coauthor of the last ICNIRP ELF blue book, part of the Static and ELF Fields EHC Task Groups at WHO, and participant in technical consultation for WHO RF research agenda in 2010. Dr. Lagroye is a member of the BioElectroMagnetics Society and European BioElectromagnetics Association.

Yann Percherancier is a cellular and molecular biochemist. During his PhD work at the Pasteur Institute (Paris, France), he studied the biochemistry of HIV-1 virus entry into T-lymphocytes, focusing on the role of specific lipid microdomains (also known as "lipid rafts") in this process. YP continued his investigations as a post-doctoral researcher in the laboratory of Michel Bouvier (University of Montreal, Quebec, Canada), recognised worldwide as a gold standard in molecular pharmacology. In October 2005, he returned to France as a CNRS staff researcher, using the BRET technique to study various cellular process in real-time on living cells. In 2009, he moved to Bordeaux and joined the Bernard Veyret research group to work on

bioelectromagnetism. His work now aims at deciphering EMF effects at the cellular and molecular level on living matter in real time.

Delia Arnaud-Cormos (M'05) was born in Cugir, Romania, in 1978. She received the Diplôme d'Ingénieur degree from the Institute of Computer Science and Communication, Rennes, France, in 2002, and the master's and Ph.D. degrees from INSA, Rennes, in 2003 and 2006, respectively. Since 2007, she has been with the Bioelectromagnetics Team, XLIM Institute, University of Limoges/C.N.R.S., Limoges, France, as an Associate Professor. In 2012, she joined the Pulsed Power Group, University of Southern California (USC), Los Angeles, SC, USA, where she developed research with the Biological Applications Research Team. Since 2018, she has been a Junior Member with the Institut Universitaire de France (IUF), Paris, France, and a member of the International Bioelectrics Consortium. Her current research interests include nanosecond pulses/microwave exposure system setup and dosimetric characterization for bioelectromagnetic studies.

Philippe Leveque (M'03) was born in Poitiers, France, in 1964. He received the Ph.D. degree from the University of Limoges, Limoges, France, in 1994. In 1995, he joined C.N.R.S. He is involved in the development of dosimetry and exposure setups for health-risk assessment in cooperation with biological and medical research groups. He is currently a Senior Scientist with CNRS and the Group Leader of Bioelectromagnetics Team with the XLIM Research Institute focusing on nanopulse application. His current research interest includes the scattering problems of electromagnetic waves, particularly in the time domain.